Published in final edited form as:

J Cell Biochem. 2017 August ; 118(8): 2241–2249. doi:10.1002/jcb.25878.

The Novel mTOR Complex 1/2 Inhibitor P529 Inhibits Human Lung Myofibroblast Differentiation

Keith T. Ferguson[1,#], **Elizabeth E. Torr**[1,#], **Ksenija Bernau**[1], **Jonathan Leet**[1], **Davis Sherris**[2], and **Nathan Sandbo**[1,*]

[1]University of Wisconsin-Madison School of Medicine and Public Health, Division of Allergy, Pulmonary, and Critical Care Medicine, 600 Highland Ave., Madison, WI 53792

[2]GenAdam Therapeutics, Inc., 37 Neillian Crescent, Jamaica Plain, MA 02130

Abstract

Idiopathic pulmonary fibrosis is a progressive and deadly disorder with very few therapeutic options. Palomid 529 (8-(1-hydroxyethyl)-2-methoxy-3-(4-methoxybenzyloxy)-benzo[c]chromen-6-one; P529) is a novel dual inhibitor of mechanistic target of rapamycin complex 1/2 (mTORC1/2). In these studies, we investigated the effect of P529 on TGF-β-dependent signaling and myofibroblast differentiation. TGF-β-induced phosphorylation of the mTORC1 targets, p70 S6 kinase 1 (S6K1) and eukaryotic translation initiation factor 4E binding protein 1 (4E-BP1), were both dose dependently inhibited by P529 in human lung fibroblasts with maximal inhibition occurring between 10–20 μM. mTORC2-mediated phosphorylation of Akt at the S473 site was partially inhibited with a similar dose dependency, as was TGF-β-induced myofibroblast differentiation. Protein levels of TGF-β-induced fibronectin and collagen were similarly decreased by P529. At this dose, there was also inhibition of mRNA transcript levels for Col1 and α-SMA, suggesting inhibition of transcriptional activation. However, there was no effect of P529 on canonical TGF-β-induced Smad signaling, as assessed by receptor-associated Smad2/3 phosphorylation, Smad2/3/4 translocation, or Smad-driven gene expression, as assessed by Smad-binding element driven luciferase. Conversely, activation of mTORC1/2 signaling was dependent on TGF-β type I receptor (ALK5) signaling and on Smad2/3 expression. P529 treatment disrupted TGF-β-induced actin stress fiber formation during myofibroblast differentiation, the deposition of new extracellular fibronectin matrix, and linear wound closure by fibroblasts. Likewise, mTOR knockdown inhibited TGF-β-induced myofibroblast differentiation. In conclusion, P529 inhibits TGF-β-induced myofibroblast differentiation, actin stress fiber formation, and matrix protein expression and deposition. Inhibition of mTORC1/2 by P529 may be a promising approach to inhibit *in vivo* fibrosis.

Keywords

actin cytoskeleton; fibronectin deposition; myofibroblast; mTOR; P529; pulmonary fibrosis; Smad; mTORC1; mTORC2; TGF-β

[*]Please address correspondence to: Nathan Sandbo, MD, Assistant Professor, University of Wisconsin-Madison School of Medicine and Public Health, Division of Allergy, Pulmonary, and Critical Care Medicine, Tel. 608-265-4576, Fax. 608-263-3104, nsandbo@medicine.wisc.edu.

[#]These authors contributed equally.

Introduction

Idiopathic pulmonary fibrosis (IPF) is a progressive fibrotic disease of the lung that leads to death within 3–5 years of diagnosis. Unfortunately, there are very few therapeutic options for treatment[Raghu et al., 2015]. Myofibroblasts are specialized, activated fibroblasts that mediate aberrant extracellular matrix (ECM) deposition during fibrosis of the lung. They are characterized by increased expression of matrix genes, along with an increased ability to assemble nascent fibronectin matrix[Torr et al., 2015]. Thus, disrupting the formation of myofibroblasts and the resulting ECM deposition is a promising strategy to halt the development of pulmonary fibrosis.

Mechanistic target of rapamycin (mTOR) is a serine/threonine kinase that is involved in regulation of translation and cell survival signaling[Huang and Fingar, 2014]. mTOR forms a complex with raptor, deptor, mammalian lethal with SEC13 protein 8 (mLST8), and proline-rich Akt substrate of 40 kDa (PRAS40) to form mTOR complex 1 (mTORC1) [Hara et al., 2002; Thedieck et al., 2007]. mTOR can also complex with rictor, deptor, mLST8, and mSIN1 to form mTOR complex 2 (mTORC2)[Frias et al., 2006; Jacinto et al., 2004; Sarbassov et al., 2004]. mTORC1 and mTORC2 have unique downstream targets. mTORC1 regulates protein synthesis and cell growth via the phosphorylation of p70 S6 kinase 1 (S6K1) and eukaryotic translation initiation factor 4E binding protein 1 (4E-BP1)[Ma and Blenis, 2009]. In contrast, mTORC2 phosphorylates Akt at Ser473, thereby regulating cell survival[Sarbassov et al., 2005; Zou et al., 2015], but it can also promote actin cytoskeletal organization[Jacinto et al., 2004; Sarbassov et al., 2004]. Previous studies that have utilized specific mTORC1 inhibitors to inhibit pulmonary fibrosis have yielded disappointing results[Malouf et al., 2011]. One potential reason for the observed lack of efficacy is that mTORC2-dependent signals may mediate downstream profibrotic effects. For instance, aberrant activation of Akt at the Ser473 residue is seen in IPF lung, suggesting a potential role for mTORC2 in the pathogenesis of this disease[Xia et al., 2008]. Furthermore, previous work in our lab has identified an important role for actin cytoskeletal reorganization in mediating myofibroblast differentiation in response to TGF-β[Sandbo and Dulin, 2011; Sandbo et al., 2011]. Thus, mTORC2-mediated effects on actin organization may be essential for the development of the myofibroblast phenotype.

Palomid 529 (8-(1-hydroxyethyl)-2-methoxy-3-(4-methoxybenzyloxy)-benzo[*c*]chromen-6-one; P529) is a novel inhibitor of mTORC1 and mTORC2 formation[Xue et al., 2008]. P529 has shown efficacy in inhibiting angiogenesis and tumor growth in experimental models via its effects on mTORC1/mTORC2[Gravina et al., 2011; Xiang et al., 2011; Xue et al., 2008]. In our studies, we examined the effect of disruption of both mTORC1 and mTORC2 by P529 on myofibroblast differentiation. We found that P529 strongly inhibited the development of the myofibroblast phenotype in response to TGF-β, resulting in strong attenuation of extracellular matrix production and deposition. These results suggest that combined disruption of mTORC1 and mTORC2 via small molecules such as P529 may be a useful strategy to disrupt fibrosis *in vivo*.

Methods

Isolation and Primary Culture of Human Pulmonary Fibroblasts

De-identified tissue samples of normal (non-fibrotic) lungs were obtained from thoracic surgical resection specimens at the Carbone Cancer Center Translational Science BioCore at the University of Wisconsin-Madison, under Institutional Review Board approval #2011-0840. Histologic assessment of the lung specimen was performed to ensure normal lung tissue architecture and absence of occult disease. Human lung fibroblasts (HLF) were isolated from resection specimens as described previously[Torr et al., 2015]. Tissue specimens were placed in DMEM with 100 U/ml streptomycin, 250 ng/ml amphotericin B, 100 U/ml penicillin, and 10 μg/ml ciprofloxacin. Alveolated lung tissue was minced, washed in PBS, and plated onto 10 cm plates in growth media containing DMEM supplemented with 10% FBS, 2 mM L-glutamine, and antibiotics as above. Expanded populations of fibroblasts were subsequently subcultured after 4 to 5 days, resulting in the development of a homogenous fibroblast population. All primary cultures were used from passage 5–10, and maintained on tissue culture plastic until the time of experiments.

Reagents

P529 was a generous gift from Palomid Pharmaceuticals Jamaica Plain, MA (now Diffusion Pharmaceuticals, Charlottesville, Virginia). TGF-β was from EMD Biosciences (616455, Gibbstown, NJ). DAPI was from Sigma-Aldrich (D9542, St. Louis, MO). Rapamycin was from LC laboratories (R-5000, Woburn, MA). Mouse monoclonal antibody against smooth muscle α-actin (α-SMA), was from Sigma-Aldrich (A5228). Mouse monoclonal antibodies against Smad2 and Akt, rabbit monoclonal antibodies against phospho-4E-BP1 (P-4E-BP1), phospho-S6K1 (P-S6K1), mTOR, phospho-mTOR (P-mTOR), phospho-Akt (P-Akt), and rabbit polyclonal antibody against phospho-Smad2 (P-Smad2), Smad3, S6K1, and 4E-BP1 were from Cell Signaling (3103, 2920, 2855, 9234, 2983, 5536, 4060, 3101, 9513, 9202, 9644, respectively, Danvers, MA). Rabbit polyclonal antibody against total fibronectin (FN) was from Abcam (ab2413, Cambridge, MA). Rabbit polyclonal antibody against collagen I (Col1) was from Cedarlane Laboratories (CL50111AP, Burlington, ON). Mouse monoclonal antibody against glyceraldehyde 3-phosphate dehydrogenase (GAPDH), Smad4, and 14-3-3 ε were from Santa Cruz Biotech (sc-32233, sc-7966, sc-23957, Santa Cruz, CA). Mouse monoclonal antibody against Lamin A/C was from BD biosciences (612162, San Jose, CA). Rhodamine phalloidin was from ThermoFisher Scientific (R415, Waltham, MA).

In vitro isolation of nuclear and cytoplasmic fractions

Preparation of nuclear and cytoplasmic fractions was performed using the NE-PER nuclear and cytoplasmic reagents (Thermo Scientific) following the manufacture's protocol and as we have done previously [Sandbo et al., 2013]. Briefly, after stimulation with desired agonists, cells were trypsinized and washed with PBS to remove trypsin by centrifugation at 300 g for 3 min. Cell pellets were suspended in cytoplasm extraction reagent for 10 min, pelleted again at 16000 g for 5 min, and the supernatant (cytoplasmic fraction) was collected. The pellets were washed and then suspended in the nuclear extraction reagent for 40 min, centrifuged at 16000g for 10 min, and the supernatant (nuclear fraction) was collected. Laemmli buffer was added and samples were boiled for 5 min prior to further

western blot analysis as described above. Immunoblotting of nuclear lamin A/C and cytoplasmic 14-3-3ε was performed to confirm the purity of the nuclear and cytoplasmic fractions, respectively.

Western Blot

After stimulation of quiescent cells with desired agonists, cells were lysed in RIPA buffer containing 25 mM HEPES (pH 7.5), 150 mM NaCl, 1% Triton X-100, 0.1% SDS, 2 mM EDTA, 2 mM EGTA, 10% glycerol, 1 mM NaF, 200 μM Na-orthovanadate, and protease inhibitor cocktail (Sigma). Cells were scraped, sonicated for 5 s and boiled in Laemmli buffer for 5 min. The samples were subjected to polyacrylamide gel electrophoresis followed by western blotting with desired primary antibodies and corresponding HRP-conjugated secondary antibodies, and developed by ECL reaction (Pierce). Digital chemiluminescent images were taken by a GE LAS4000 chemiluminescence imager. Densitometry was performed using *ImageJ* [Schneider et al., 2012].

Immunofluorescence Staining

Cells were washed twice with TBS, fixed with 4% paraformaldehyde/TBS for 30 min at room temperature (RT) and then permeabilized with 0.2% Triton X-100/TBS for 5 min at RT. Cells were then blocked with 10% Normal Goat Serum (NGS), 1% BSA in TBS for 1 h at RT and incubated overnight with the desired primary antibody at 4°C. Cells were washed with TBS and incubated with the corresponding rhodamine or fluorescein (FITC) conjugated secondary antibody for 75 min at 37°C, washed, incubated with DAPI/TBS (0.42 μg/ml) for 10 min at RT, washed and mounted using Ibidi mounting media (Munich, Germany). Immunofluorescent images were obtained using an Olympus 1X71 fluorescent microscope and Q imaging Retiga 2000R camera.

Reverse Transcription Quantitative Real Time PCR

Real time PCR was carried out as before [Sandbo et al., 2013]. Real time PCR primers:

α-SMA:

AAAGACAGCTACGTGGGTGACGAA (forward)

TTCCATGTCGTCCAGTTGGTGAT (reverse)

Col1a1:

CCAGAAGAACTGGTACATCAGCA (forward)

CGCCATACTCGAACTGGAAT (reverse).

FN:

GAGTGTGTGTGTCTTGGTAATGG (forward)

CCACGTTTCTCCGACCAC (reverse)

PAI1:

GAGACAGGCAGCTCGGATTC (forward)

GGCCTCCCAAAGTGCATTAC (reverse)

siRNA Knockdown Assays

Prior to transfection, HLF were plated at 5 × 104 cells/ml for 24 h reaching 70–80% confluency by the time of transfection. siRNA (Qiagen, Valencia, CA) was transfected using RNAiMAX transfection reagent (13778, Life Technologies) diluted in Opti-MEM (31985062, Gibco Life Technologies) with 1 μl RNAiMAX per 10 pmol of siRNA. Pre-determined concentrations of siRNA were used to achieve sufficient knock-down. Cells were incubated for 24 h, serum starved, stimulated as indicated and cell lysates were analyzed using gel electrophoresis followed by Western blotting. All siRNA sequences were from Qiagen.

siRNA Sequences

All siRNA sequences were from Qiagen and included: Allstars 1 (scrambled, SI03650318), human Smad2-7 sequence AAGAGGAGTGCGCTTATACTA (SI03031875), human Smad3-3 sequence AAGAGATTCGAATGACGGTAA (SI00082495), human mTOR-5 SI00300244 sequence ACTCGCTGATCCAAATGACAA.

DNA Transfection and Luciferase Reporter Assay

HLF were plated at 5×10^4 cells/ml and incubated overnight in growth media. Transient DNA transfections were performed using GenJet reagent (SL100488, SignaGen Laboratories, Gaithersburg, MD) following the standard manufacturer's instructions. Cells were co-transfected with 1 μg of firefly luciferase reporter plasmid and 200 ng of constitutively active thymidine kinase promoter-Renilla luciferase reporter plasmid. Cells were placed in growth media overnight and then serum-starved for 24 h, followed by stimulation with the desired agonists for the time points indicated in the figure legends. Cells were then washed with PBS and lysed in protein extraction reagent (78501, Thermo Fisher). The lysates were assayed for firefly and Renilla luciferase activity using the Dual-Luciferase assay kit (E1960, Promega, Madison, WI).

Linear Wound Migration Assay

HLF were plated at a density of 5×10^4 cells/ml into 6-well plates that had been scored with a razor blade to provide reference locations for imaging. Cells were allowed to grow to confluency in serum containing media for 48 h. Thirty min prior to wounding, media was changed to serum-free media containing 0.1% bovine serum albumin. Cells were treated at that time with either 10 μM P529 or vehicle control. Three linear wounds were made in the confluent monolayer of each well with a pipette tip, and the wound closure was measured 24 h after wound creation. Microscope images were obtained at a 10X magnification at time 0 and time 24 from nine pre-determined, marked locations. Images were assembled using Photoshop 7.0 program. Analysis of the area of the remaining wound in each image was performed using *ImageJ* software. Cell edges were enhanced using *ImageJ* edge function. For presentation the black/white image was inverted and contrast enhanced. Values were expressed as percent wound closure: $100 \times (1\text{-}\text{Area}_{t=24}/\text{Area}_{t=0})$.

Statistical analysis

Differences between treatment conditions were assessed via the Student's t-test and deemed statistically significant at an α level of 5% ($p<0.05$).

Results

P529 inhibits both mTORC1 and mTORC2

We first explored whether P529 inhibited mTOR dependent pathways during myofibroblast differentiation induced by TGF-β. As shown in Fig. 1A, treatment with 1 ng/ml of TGF-β for 24 hours induces phosphorylation of S6K1 and 4E-BP1, both known targets of mTORC1. P529 dose-dependently inhibited TGF-β-induced phosphorylation of S6K1 at T389 and 4E-BP1 at T37/46, with significant inhibition occurring at 10 μM, as quantified in Figure 1E. Likewise, TGF-β-induced phosphorylation of the S2448 residue on mTOR, a downstream target of S6K1[Chiang and Abraham, 2005], was dose dependently inhibited by P529. In total, these results confirm the efficacy of P529 as an mTORC1 inhibitor in this context. We then assessed whether P529 could inhibit mTORC2 activity. As shown in Fig. 1B, induction of phosphorylation of Akt at the S473 residue, a known target of mTORC2, was significantly inhibited by P529 with a similar dose dependency. Significant inhibition of TGF-β-induced P-Akt (S473) occurred at 10 μM (Fig. 1C). In contrast, whereas treatment with rapamycin resulted in a similar degree of inhibition of P-4E-BP1 and P-S6K1, it did not inhibit TGF-β-induced P-Akt suggesting that rapamycin had no effect on mTORC2-dependent signaling (Fig. 1D, 1E). Overall, these results show that P529 has the ability to inhibit both mTORC1 and mTORC2 activation by TGF-β.

mTORC1/2 is required for myofibroblast differentiation

We then examined the effect of mTORC1/2 inhibition by P529 on induction of the myofibroblast marker, smooth muscle α-actin (α-SMA), and ECM genes in response to TGF-β. As shown in Figs. 2A, 2B, treatment with P529 dose-dependently inhibited TGF-β-induced FN, Col1, and α-SMA, with maximal inhibition occurring at 10 μM. This concentration was the same as where significant inhibition of mTORC1/2 occurred (Fig. 1). Similarly, treatment with P529 attenuated TGF-β-dependent increases in α-SMA and Col1 mRNA (Fig. 2C), suggesting possible regulation of transcriptional activity. Interestingly, P529 did not attenuate all TGF-β-inducible genes. FN showed a trend toward decreased TGF-β-induced expression under treatment with P529, but this result was not statistically significant ($p=0.11$). In contrast, P529 significantly attenuated mRNA for extra-domain type III containing fibronectin (EDA-FN) (data not shown). P529 did not attenuate either TGF-β-induced plasminogen activator inhibitor 1 (PAI-1) mRNA, or periostin (data not shown). These data suggest that there is differential inhibition of mRNA expression, which may suggest inhibition of specific transcriptional mediators.

P529 effects are downstream of Smad-signaling

To determine whether P529 could be affecting TGF-β receptor-mediated signaling, we assessed its effect on Smad signaling. As shown in Fig. 3A & 3B, TGF-β-induced Smad2 phosphorylation was not affected by incubation with increasing doses of P529. Activation of

Smad-dependent transcription in response to TGF-β requires translocation of the Smad2/3/4 complex [Hu et al., 2003; Massague, 2000; Sandbo et al., 2013]. Under treatment with P529, we did not see any disruption of Smad2/3/4 translocation in response to stimulation with TGF-β (Figure 3C, D). Likewise, P529 had no effect on Smad-mediated luciferase activity (Fig. 3E). Conversely, treatment with the TGF-β type 1 receptor kinase (ALK5) inhibitor, SB542531, did inhibit S6K1 phosphorylation (Fig. 3F,G). Similarly, siRNA-mediated knockdown of Smad2 or Smad3 resulted in loss of TGF-β-mediated S6K1 phosphorylation (Fig. 3H, I). This demonstrated that activation of mTORC1/2 requires intact TGF-β type 1 receptor (ALK5) signaling via Smad2/3. Finally, we assessed the expression level of Smad7, which can inhibit the profibrotic signaling by TGF-β[Yan et al., 2016]. There was no effect of P529 on Smad7 expression under basal or TGF-β stimulated conditions (data not shown). Overall, from these findings we conclude that signaling via mTORC1/2 is downstream of the TGF-β type I receptor (ALK5) and Smad2/3. As a result, disrupting mTORC1/2 by P529 does not impact TGF-β type I receptor-mediated Smad-signaling.

P529 inhibits actin stress fiber formation and fibronectin deposition

Given its lack of effect on Smad-signaling, we sought to further understand how P529 may be inhibiting the development of the myofibroblast phenotype. Reorganization of cytosolic actin into stress fibers is an essential feature of the myofibroblast phenotype and plays a role in transcriptional regulation of myofibroblast associated genes[Sandbo and Dulin, 2011; Sandbo et al., 2011]. mTORC2 has been implicated in actin polymerization[Jacinto et al., 2004], but its effect on the formation of actin stress fibers during myofibroblast differentiation has not been examined. Phalloidin staining of actin filaments in cells treated with TGF-β demonstrated that TGF-β strongly induced the formation of actin stress fibers (Fig. 4A, middle panel). Incubation with P529 significantly attenuated stress fiber formation (Fig. 4A, right panel), suggesting that mTORC2 may play an essential role in their formation during myofibroblast differentiation. Actin polymerization and the formation of a contractile phenotype is a prerequisite for both myofibroblast differentiation[Sandbo et al., 2011] and the formation of nascent extracellular fibronectin matrix by fibroblasts[Torr et al., 2015; Zhang et al., 1997]. Given the observed disruption in actin stress fiber formation, we then examined the deposition of fibronectin by fibroblasts in response to TGF-β under treatment with P529. HLF stimulated with TGF-β have a significant increase in the amount of extracellular fibronectin fibrils observed by immunofluorescent staining (Fig. 4B, middle panels). Treatment with P529 attenuated the observed formation of extracellular fibrils (Fig. 4B, right panels), consistent with the observed effects on myofibroblast differentiation and fibronectin expression.

As an alternative approach, we utilized siRNA-mediated knockdown of mTOR to determine the role of mTORC1/2 in myofibroblast differentiation. As shown in Figure 4C, siRNA-mediated loss of mTOR results in loss of mTOR-dependent signaling (S6 kinase phosphorylation), as expected. Additionally, loss of mTOR expression also results in inhibition of TGF-β-induced myofibroblast differentiation (as assessed by expression of the myofibroblast marker, α-SMA (Fig. 4C and 4D)). These results are consistent with the results we see with pharmacologic inhibition by P529, suggesting an essential role for

mTOR complexes (mTORC1 and mTORC2) in mediating myofibroblast differentiation in response to TGF-β.

Finally, because of the important role of the actin cytoskeletal organization in mediating cell motility[Lauffenburger and Horwitz, 1996], we examined if fibroblast migration in response to a wound would be affected by P529. As shown in Fig. 4E and 4F, treatment with P529 significantly delayed linear wound closure, compared to untreated cells, suggesting that loss of actin filament formation (Figure 4A) may translate to disrupted migration. This suggests that P529 may inhibit wound repair by an additional mechanism during tissue fibrosis.

Discussion

In these studies, we have found that the novel small molecule, P529, is an effective inhibitor of both mTORC1 and mTORC2 in primary cultures of HLF. We have further found that dual inhibition of mTORC1/2 disrupts formation of the myofibroblast phenotype in response to TGF-β. Treatment with P529 strongly inhibited the protein expression of the myofibroblast marker, α-SMA, but also the expression of extracellular matrix genes such as FN and Col1. Novel findings from our study include an observed loss of α-SMA and Col1 transcript levels, attenuation of actin stress fiber formation and fibronectin deposition, and loss of migratory capacity in cells treated with P529. These results suggest a potential role for P529 as an antifibrotic agent *in vivo*.

Given the known role of mTORC1 in exerting control on cap-dependent translation via 4E-BP1[Hara et al., 2002; Ma and Blenis, 2009], some loss of protein expression may be expected in response to a TORC1/2 inhibitor such as P529. Indeed, we observed that P529 significantly attenuated TGF-β-induced FN expression at the protein level but did not significantly attenuate FN mRNA, consistent with an effect on translational regulation. However, treatment with P529 also resulted in decreased levels of α-SMA and Col1 mRNA in response to TGF-β. This suggests that for α-SMA and Col1, regulation of transcription activation may have played an important role in modifying protein expression, rather than global changes in translational activity. We observed that activation of TORC1-dependent signals require TGF-β type I receptor signaling via Smad 2/3. However, we did not observe an effect of P529 on TGF-β-induced Smad2 phosphorylation, Smad 2/3/4 translocation, or Smad-driven gene expression. Thus, P529-induced changes in transcriptional activity would need to be downstream of TGF-β-mediated Smad signaling. Taken together, these data suggests that the inhibition of mTORC2 by P529 may regulate transcription of profibrotic genes, in addition to the effect of mTORC1 on protein translation.

One potential mechanism by which mTORC2 could affect transcriptional regulation downstream of Smad-signaling would be via its effects on the actin cytoskeleton. Our group has previously shown that myofibroblast differentiation requires actin stress fiber formation, via modulation of megakaryoblastic leukemia 1/serum response factor (MKL1/SRF) activity[Sandbo et al., 2009; Sandbo et al., 2011]. Inhibition of mTORC2 with P529 results in a marked attenuation of actin stress fiber formation, suggesting a putative mechanism by which myofibroblast differentiation could be attenuated. From a functional standpoint, P529-induced loss of actin stress fiber formation and myofibroblast differentiation was

associated with a reduction in deposited extracellular FN. Extracellular fibrillar FN is required for the binding of other ECM proteins, and thus serves as a scaffold for new ECM formation[Sottile and Hocking, 2002; Torr et al., 2015]. Thus, therapies that disrupt the formation of nascent extracellular matrix may be important for treating pulmonary fibrosis.

This work demonstrates that dual inhibition of mTORC1/2 may be an attractive target for therapeutic intervention in pulmonary fibrosis. mTOR expression has been associated with higher levels of fibrosis and pulmonary function decline[Park et al., 2014] and is associated with mesenchymal cell activation and collagen expression[Walker et al., 2016]. Our work in primary cultures of HLF shows that inhibition of mTORC1/2 by P529 inhibits development of the myofibroblast phenotype in response to the profibrotic cytokine, TGF-β. In addition, we observed disruption of fibronectin extracellular matrix and fibroblast migration by treatment with P529, suggesting that P529 may have additional antifibrotic effects. Disappointingly, previous studies using the mTORC1 inhibitor everolimus did not show significant benefit in treating idiopathic pulmonary fibrosis[Malouf et al., 2011]. The antifibrotic effect of mTORC1-inhibitors may be have been limited by the lack of inhibition of mTORC2, which has its own distinct downstream signaling targets. Supporting this notion, recent preclinical studies have found that mTORC2 is important in mediating pulmonary fibrosis[Chang et al., 2014]. Our studies, using P529, a novel small molecule inhibitor of formation of mTORC1/2, build upon this previous work, strengthening the evidence that mTORC2 mediates critical cell functions important for the development of pulmonary fibrosis. As the studies presented here are based in cell culture models of fibroblast activation, future studies will need to be performed in animal models of pulmonary fibrosis to determine the potential efficacy of P529 *in vivo*.

In summary, we have found that dual inhibition of mTORC1/2 by the novel small molecule P529 strongly inhibits the development of myofibroblast differentiation and deposition of nascent ECM. This suggests that this may be a promising approach to modify the development of fibrosis *in vivo*.

Acknowledgments

This study was supported by National Institutes of Health Awards K08 HL093367 (NS) and University of Wisconsin-Madison Development funding (NS). Human lung fibroblasts were derived from de-identified tissue samples from thoracic surgical resection specimens obtained by the Carbone Cancer Center Translational Science BioCore at the University of Wisconsin-Madison, under IRB approval #2011-0840. This work is supported in part by NIH/NCI P30 CA014520-UW Comprehensive Cancer Center. We thank David Sherris, Ph. D. and RestorGenex, Inc. for supplying P529 and vehicle. KF, KB, ET, JL, and NS have no conflict of interest to declare. DS holds stock in Diffusion Pharmaceuticals (previously Palomid Pharmaceuticals).

References

Chang W, Wei K, Ho L, Berry GJ, Jacobs SS, Chang CH, Rosen GD. A critical role for the mTORC2 pathway in lung fibrosis. PloS one. 2014; 9:e106155. [PubMed: 25162417]

Chiang GG, Abraham RT. Phosphorylation of mammalian target of rapamycin (mTOR) at Ser-2448 is mediated by p70S6 kinase. The Journal of biological chemistry. 2005; 280:25485–90. [PubMed: 15899889]

Frias MA, Thoreen CC, Jaffe JD, Schroder W, Sculley T, Carr SA, Sabatini DM. mSin1 is necessary for Akt/PKB phosphorylation, and its isoforms define three distinct mTORC2s. Current biology : CB. 2006; 16:1865–70. [PubMed: 16919458]

Gravina GL, Marampon F, Petini F, Biordi L, Sherris D, Jannini EA, Tombolini V, Festuccia C. The TORC1/TORC2 inhibitor, Palomid 529, reduces tumor growth and sensitizes to docetaxel and cisplatin in aggressive and hormone-refractory prostate cancer cells. Endocrine-related cancer. 2011; 18:385–400. [PubMed: 21551258]

Hara K, Maruki Y, Long X, Yoshino K, Oshiro N, Hidayat S, Tokunaga C, Avruch J, Yonezawa K. Raptor, a binding partner of target of rapamycin (TOR), mediates TOR action. Cell. 2002; 110:177–89. [PubMed: 12150926]

Hu B, Wu Z, Phan SH. Smad3 mediates transforming growth factor-beta-induced alpha-smooth muscle actin expression. Am J Respir Cell Mol Biol. 2003; 29:397–404. [PubMed: 12702545]

Huang K, Fingar DC. Growing knowledge of the mTOR signaling network. Seminars in cell & developmental biology. 2014; 36:79–90. [PubMed: 25242279]

Jacinto E, Loewith R, Schmidt A, Lin S, Ruegg MA, Hall A, Hall MN. Mammalian TOR complex 2 controls the actin cytoskeleton and is rapamycin insensitive. Nature cell biology. 2004; 6:1122–8. [PubMed: 15467718]

Lauffenburger DA, Horwitz AF. Cell migration: a physically integrated molecular process. Cell. 1996; 84:359–69. [PubMed: 8608589]

Ma XM, Blenis J. Molecular mechanisms of mTOR-mediated translational control. Nature reviews Molecular cell biology. 2009; 10:307–18. [PubMed: 19339977]

Malouf MA, Hopkins P, Snell G, Glanville AR. An investigator-driven study of everolimus in surgical lung biopsy confirmed idiopathic pulmonary fibrosis. Respirology. 2011; 16:776–83. [PubMed: 21362103]

Massague J. How cells read TGF-beta signals. Nature reviews Molecular cell biology. 2000; 1:169–78. [PubMed: 11252892]

Park JS, Park HJ, Park YS, Lee SM, Yim JJ, Yoo CG, Han SK, Kim YW. Clinical significance of mTOR, ZEB1, ROCK1 expression in lung tissues of pulmonary fibrosis patients. BMC pulmonary medicine. 2014; 14:168. [PubMed: 25358403]

Raghu G, Rochwerg B, Zhang Y, Garcia CA, Azuma A, Behr J, Brozek JL, Collard HR, Cunningham W, Homma S, Johkoh T, Martinez FJ, Myers J, Protzko SL, Richeldi L, Rind D, Selman M, Theodore A, Wells AU, Hoogsteden H, Schunemann HJ. An Official ATS/ERS/JRS/ALAT Clinical Practice Guideline: Treatment of Idiopathic Pulmonary Fibrosis. An Update of the 2011 Clinical Practice Guideline. American journal of respiratory and critical care medicine. 2015; 192:e3–19. [PubMed: 26177183]

Sandbo N, Dulin N. Actin cytoskeleton in myofibroblast differentiation: ultrastructure defining form and driving function. Translational research : the journal of laboratory and clinical medicine. 2011; 158:181–96. [PubMed: 21925115]

Sandbo N, Kregel S, Taurin S, Bhorade S, Dulin NO. Critical role of serum response factor in pulmonary myofibroblast differentiation induced by TGF-beta. Am J Respir Cell Mol Biol. 2009; 41:332–8. [PubMed: 19151320]

Sandbo N, Lau A, Kach J, Ngam C, Yau D, Dulin NO. Delayed stress fiber formation mediates pulmonary myofibroblast differentiation in response to TGF-beta. American journal of physiology Lung cellular and molecular physiology. 2011; 301:L656–66. [PubMed: 21856814]

Sandbo N, Ngam C, Torr E, Kregel S, Kach J, Dulin N. Control of myofibroblast differentiation by microtubule dynamics through a regulated localization of mDia2. The Journal of biological chemistry. 2013; 288:15466–73. [PubMed: 23580645]

Sarbassov DD, Ali SM, Kim DH, Guertin DA, Latek RR, Erdjument-Bromage H, Tempst P, Sabatini DM. Rictor, a novel binding partner of mTOR, defines a rapamycin-insensitive and raptor-independent pathway that regulates the cytoskeleton. Current biology : CB. 2004; 14:1296–302. [PubMed: 15268862]

Sarbassov DD, Guertin DA, Ali SM, Sabatini DM. Phosphorylation and regulation of Akt/PKB by the rictor-mTOR complex. Science. 2005; 307:1098–101. [PubMed: 15718470]

Schneider CA, Rasband WS, Eliceiri KW. NIH Image to ImageJ: 25 years of image analysis. Nature methods. 2012; 9:671–5. [PubMed: 22930834]

Sottile J, Hocking DC. Fibronectin polymerization regulates the composition and stability of extracellular matrix fibrils and cell-matrix adhesions. Molecular biology of the cell. 2002; 13:3546–59. [PubMed: 12388756]

Thedieck K, Polak P, Kim ML, Molle KD, Cohen A, Jeno P, Arrieumerlou C, Hall MN. PRAS40 and PRR5-like protein are new mTOR interactors that regulate apoptosis. PloS one. 2007; 2:e1217. [PubMed: 18030348]

Torr EE, Ngam CR, Bernau K, Tomasini-Johansson B, Acton B, Sandbo N. Myofibroblasts exhibit enhanced fibronectin assembly that is intrinsic to their contractile phenotype. The Journal of biological chemistry. 2015; 290:6951–61. [PubMed: 25627685]

Walker NM, Belloli EA, Stuckey L, Chan KM, Lin J, Lynch W, Chang A, Mazzoni SM, Fingar DC, Lama VN. Mechanistic Target of Rapamycin Complex 1 (mTORC1) and mTORC2 as Key Signaling Intermediates in Mesenchymal Cell Activation. The Journal of biological chemistry. 2016; 291:6262–71. [PubMed: 26755732]

Xia H, Diebold D, Nho R, Perlman D, Kleidon J, Kahm J, Avdulov S, Peterson M, Nerva J, Bitterman P, Henke C. Pathological integrin signaling enhances proliferation of primary lung fibroblasts from patients with idiopathic pulmonary fibrosis. The Journal of experimental medicine. 2008; 205:1659–72. [PubMed: 18541712]

Xiang T, Jia Y, Sherris D, Li S, Wang H, Lu D, Yang Q. Targeting the Akt/mTOR pathway in Brca1-deficient cancers. Oncogene. 2011; 30:2443–50. [PubMed: 21242970]

Xue Q, Hopkins B, Perruzzi C, Udayakumar D, Sherris D, Benjamin LE. Palomid 529, a novel small-molecule drug, is a TORC1/TORC2 inhibitor that reduces tumor growth, tumor angiogenesis, and vascular permeability. Cancer research. 2008; 68:9551–7. [PubMed: 19010932]

Yan X, Liao H, Cheng M, Shi X, Lin X, Feng XH, Chen YG. Smad7 Protein Interacts with Receptor-regulated Smads (R-Smads) to Inhibit Transforming Growth Factor-beta (TGF-beta)/Smad Signaling. The Journal of biological chemistry. 2016; 291:382–92. [PubMed: 26555259]

Zhang Q, Magnusson MK, Mosher DF. Lysophosphatidic acid and microtubule-destabilizing agents stimulate fibronectin matrix assembly through Rho-dependent actin stress fiber formation and cell contraction. Mol Biol Cell. 1997; 8:1415–25. [PubMed: 9285815]

Zou Z, Chen J, Liu A, Zhou X, Song Q, Jia C, Chen Z, Lin J, Yang C, Li M, Jiang Y, Bai X. mTORC2 promotes cell survival through c-Myc-dependent up-regulation of E2F1. The Journal of cell biology. 2015; 211:105–22. [PubMed: 26459601]

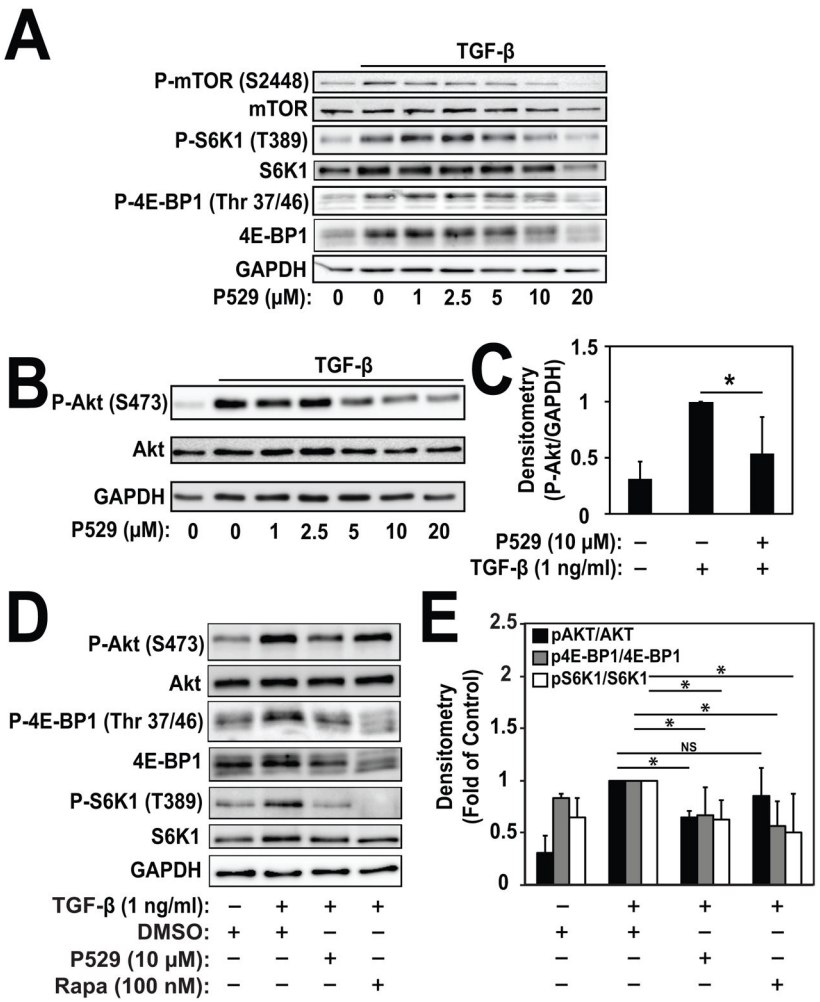

Fig. 1. P529 inhibits TGF-β-induced mTOR signaling, but not Smad-signaling in HLF

HLF were treated with 1 ng/mL TGF-β for 24 hours in the presence of the indicated concentrations of P529. N=3 biologic repeats. **A)** Western blot of whole cell lysates showing inhibition of TGF-β-induced P-mTOR (S2448), P-S6K1 (T389), and P-4E-BP1 (Thr 37/46) by P529. **B)** Western blot of whole cell lysates and **C)** quantitation of indicated proteins showing dose-dependent inhibition of TGF-β-induced P-Akt (S473) by P529. Statistical significance was tested using student's t-test. ***** denotes statistically significant differences (p<0.05) between P-Akt levels in the TGF-β and TGF-β/P529 treatment conditions. **D)** Western blot of whole cell lysates showing inhibition of TGF-β-induced P-Akt (S473) by P529, but not rapamycin. **E)** Quantitation of P-Akt/Akt, P-4E-BP1/4E-BP1 and P-S6K1/S6K1 blots by densitometry. Statistical significance was tested using student's t-test. ***** denotes statistically significant differences (p<0.05). NS denotes not significant.

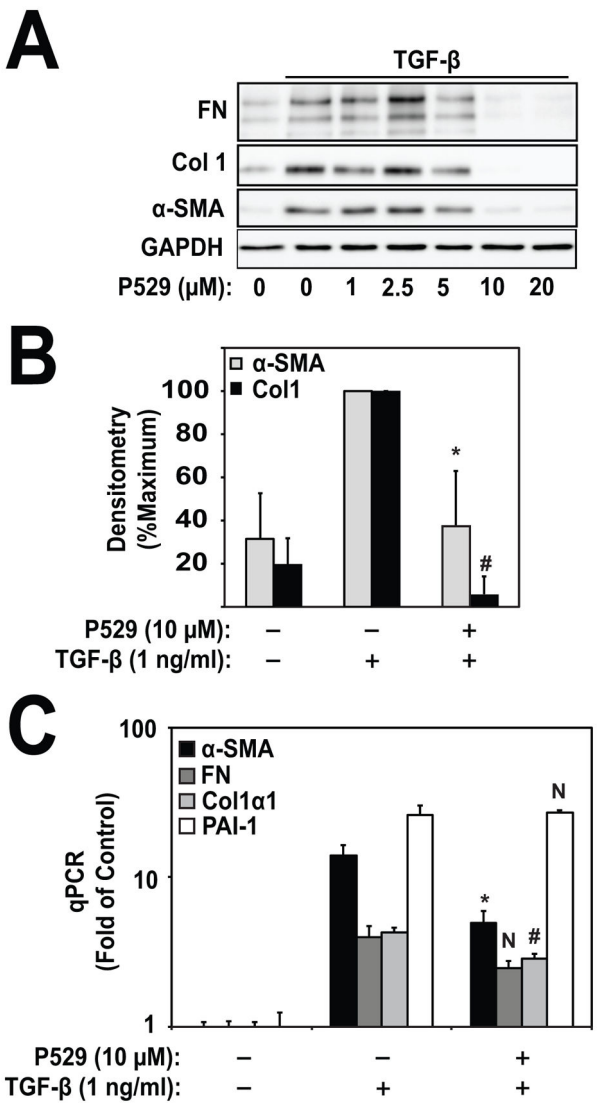

Figure 2. P529 Inhibits myofibroblast differentiation

A) HLF were treated with 1 ng/ml TGF-β for 24 h and the indicated concentrations of P529. Lysates were subjected to western blotting for α-SMA, collagen-1, fibronectin, and GAPDH. N=3 biologic repeats. **B)** Densitometry of Col1/GAPDH and α-SMA/GAPDH. Measurements are normalized to the TGF-β treatment condition. Statistical significance was tested using student's t-test. *, # denote statistically significant differences ($p<0.05$) between expression of α-SMA (*) or Col1 (#) in the TGF-β and TGF-β/P529 treatment conditions. **C)** Real time PCR of the indicated genes. Statistical significance was tested using student's t-test. *, # denote statistically significant differences ($p<0.05$) between expression of α-SMA (*) or Col1 (#) in the TGF-β and TGF-β/P529 treatment conditions. N, denotes not statistically significant (FN and PAI-1).

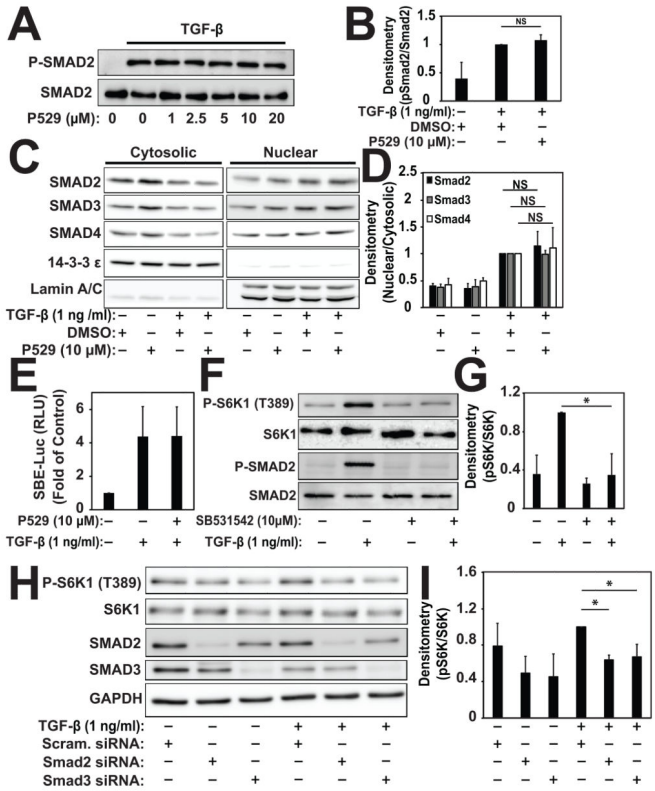

Fig. 3. P529 has no effect on TGF-β-induced Smad signaling

A, B) HLF were treated with 1 ng/mL TGF-β for 30 min in the presence of the indicated concentrations of P529 followed by western blotting of cell lysates and densitometry for the indicated (phospho) proteins. Statistical significance was tested using student's t-test. NS denotes a non-significant differences (p>0.05) between conditions. **C, D)** HLF were treated with 1 ng/mL TGF-β for 2 h in the presence of the indicated concentrations of 10 μM P529 or vehicle control. Nuclear and cytosolic extracts were prepared as and subjected to western blotting for the indicated proteins, followed by densitometry. Statistical significance was tested using student's t-test. NS denotes a non-significant differences (p>0.05) between conditions. **E)** HLF were transiently transfected with Smad-binding element driven luciferase, treated with TGF-β for 24 h in the presence of P529 or vehicle control, followed by assessment of cell lysates for luciferase activity. N=4 biologic repeats. **F, G)** HLF were treated with 1 ng/mL TGF-β for 24 h in the presence of the indicated concentrations of the ALK5 inhibitor SB531542 or vehicle control. Total cell lysates were subjected to western blotting for the indicated (phospho) proteins, followed by densitometry of the indicated bands. Statistical significance was tested using student's t-test. * denote statistically significant differences (p<0.05) between conditions. **H, I)** HLF were transfected with siRNA targeting Smad2, Smad3, or scrambled control, followed by treatment with 1 ng/ml TGF-β for 24 h, followed by western blotting and densitometry of the indicated proteins. Statistical significance was tested using student's t-test. * denote statistically significant differences (p<0.05) between the indicated conditions.

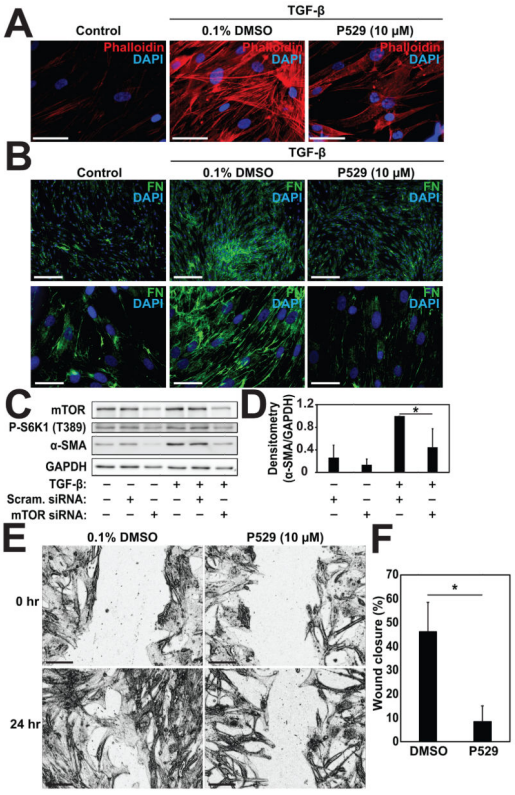

Figure 4. P529 inhibits TGF-β-induced actin stress fiber formation and fibronectin deposition into the ECM

HLF were treated with 1 ng/ml TGF-β for 24 h and P529 or vehicle control, as indicated. **A)** Cells were then subjected to staining with phalloidin (red) and DAPI (Blue) and visualized with a 60x objective. Scale bar = 50 μm. **B)** Cells were stained with anti-fibronectin antibody (green) and DAPI (Blue) and visualized with a 10x objective (top row) or a 60x objective (bottom row). Scale bar = 250 μm. **C, D)** HLF were transfected with siRNA targeting mTOR or scrambled control, followed by treatment with 1 ng/ml TGF-β for 24 h, followed by western blotting and densitometry of the indicated proteins. Statistical significance was tested using student's t-test. * denote statistically significant differences (p<0.05) between conditions. **E)** HLF were plated and grown overnight on tissue culture plastic. Serum-free media with DMSO or 10 μM P529 was then added to induce growth arrest. Linear wounds were made at the time of serum removal and imaged. Cells were fixed after 24 h and imaged with a 10x objective. Images shown have been processed with *ImageJ* to enhance edges and contrast for clarity. **F)** Closure after 24 h was measured using Image J. Scale Bar = 200 μM. Statistical significance was tested using student's t-test. * denote statistically significant differences (p<0.05) between conditions.